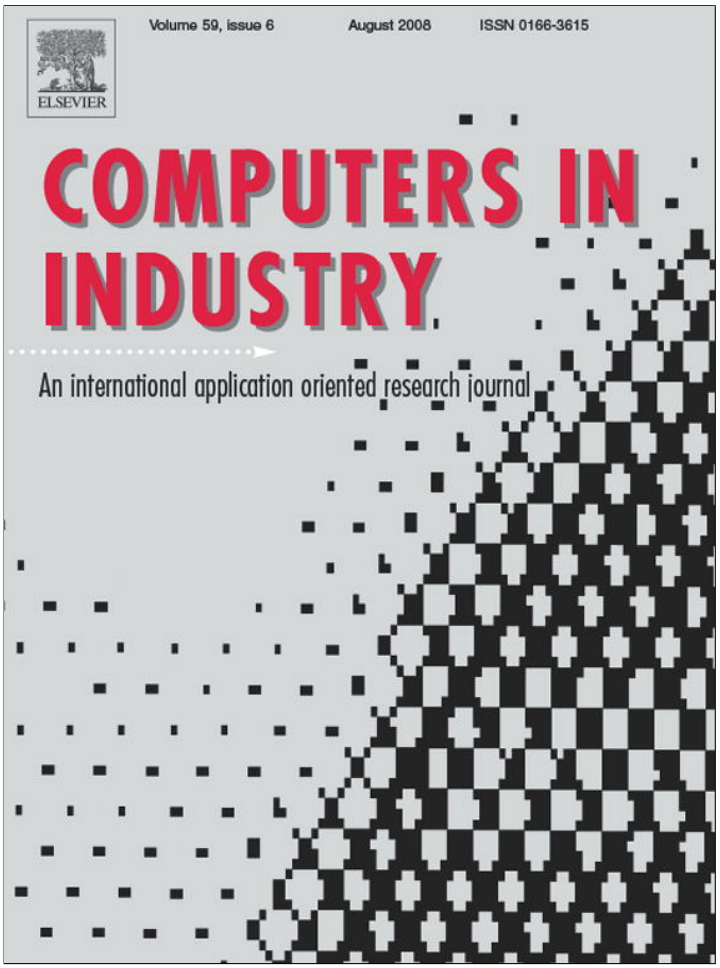

Computers in Industry 59 (2008) 601–611

Contents lists available at ScienceDirect

Computers in Industry

journal homepage: www.elsevier.com/locate/compind

Computer aided geometric design of strip using developable Bézier patches

Chih-Hsing Chu [a,*], Charlie C.L. Wang [b], Chi-Rung Tsai [a]

[a] Department of Industrial Engineering and Engineering Management, National Tsing Hua University, Hsinchu, Taiwan
[b] Department of Computer Aided Engineering and Automation, The Chinese University of Hong Kong, Shatin N.T., Hong Kong, China

ARTICLE INFO

Article history:
Received 7 April 2007
Received in revised form 31 January 2008
Accepted 9 March 2008
Available online 28 April 2008

Keywords:
Developable strip
Bézier patch
Computer-aided geometric design
Shape design

ABSTRACT

Developable strip is commonly used in product design due to its ease of manufacture. This paper proposes an algorithm for geometric design of strip using developable Bézier patches. It computes an aggregate of triangular and quadrilateral patches interpolate two given space curves defining a strip. The computation process selects optimal solutions in terms of surface assessment criteria specified by the user. Each patch is then degree-elevated to gain extra degrees of freedom, which produce G1 across the patch boundaries by modifying the control points while preserving the surface developability. Test examples with different design parameters illustrate and validate the feasibility of the proposed algorithm. In comparison with previous studies, this work allows strip design with freeform developable patches, generates better results in the surface assessment, and provides more flexible control on the design shape. It serves as a simple but effective approach for computer aided geometric design of developable strip.

1. Introduction

Developable surfaces are a subset of ruled surfaces which can be unfolded (or developed) into a plane without tearing or stretching during the process. This property, known as the developability, eases manufacture of 3D objects. Hence, developable shapes are widely used in industries such as sheet metal forming [1], ship building [2,3], windshield design, and fabrication of apparels including shoes and clothing [4,5]. Parts are first modeled with developable strips in space. They are then flattened into a planner pattern. The manufacturing process starts with cutting a material according to the pattern. Unrolling the cut material simply resumes its original 3D shape. A final step is often applied to assemble different pieces by welding or sewing in order to form the final product.

There have been two different approaches proposed for CAGD of a single developable surface. The first approach represents a surface as a tensor product of degree $(1, n)$ with non-linear constraints imposed by the developability. The user can thus control the shape in a very limited manner, e.g. some but not all of the control points. The remaining parameters must be solved from the constrained system [6–11]. Instead, one can treat a developable surface as an envelope of one parameter set of tangent planes. The surface becomes a curve in dual projective space [12]. Design methods were proposed for Bézier and B-spline surfaces based on the duality theory [13,14]. However, they may be lacking of practicality in CAGD applications.

Many engineering products consist of double-curved surfaces, which are not perfectly developable. It is thus necessary to allow certain deviations in the developability. Several studies have developed CAGD methods that approximate 3D shape using developable surfaces. Some concerned with interpolation and approximation algorithms based on the dual approach [15–19]. Leopoldseder and Pottmann [16] modeled a given developable surface by surfaces of revolution. Each pair of consecutive rulings and tangent planes that approximates the given surface is interpolated by smoothly linked circular cones. Their later work allowed a point cloud as the input for applications in reverse engineering [17,18]. On the other hand, several literatures [20,21,22–24] were focused on increasing the developability of a strip in the tessellation representation. Wang et al. [20] proposed a function optimization method for increasing the developability of a trimmed NURBS surface by adjusting the positions and weights of the surface control points. Tang and Wang [22] introduced a modeling algorithm that interpolates a strip defined by two given

* Corresponding author at: Department of Industrial Engineering and Engineering Management, National Tsing Hua University, 101 Kuang Fu Road, Section 2, Hsinchu, Taiwan.
E-mail addresses: chchu@ie.nthu.edu.tw (C.-H. Chu), cwang@acae.cuhk.edu.hk (C.-R. Tsai).

0166-3615/$ – see front matter © 2008 Elsevier B.V. All rights reserved.
doi:10.1016/j.compind.2008.03.001

space curves with an aggregate of triangles. The interpolation task was formulated as a variant of boundary triangulations and thus transformed into the shortest-path problem [23]. Their later work [24] optimized the result based on various objective functions considering different CAD/CAM applications.

Strip design using developable surfaces possesses a wide range of industrial applications. It is commonly used in design and manufacture of sheet metal parts and apparel. Developable strip design has recently found novel applications such as generation of tool path in five-axis flank milling [25], simulation of robot motions [26], and fabrication of sculptures in art [27]. However, the past studies fail to provide geometric design methods that balance the modeling capability and usability in practice. This paper introduces a greedy algorithm for CAGD of strip with freeform developable patches. It calculates consecutive quadratic Bézier patches in the conical form, consisting of triangular and quadrilateral patches, that interpolates two given boundary curves in space. Simple heuristics are applied to select one optimal solution in terms of surface evaluation criteria among the feasible patches starting with a ruling defined by two sampling points from the curves. The patches generated connect with only positional continuity. The next step is to perform degree elevation on each patch. The resultant cubic patch provides extra degrees of freedom in the strip design. G1 continuity is thus produced across the degree-elevated patches by adjusting their control polygons while maintaining the surface developability. Test strips defined by highly convoluted curves demonstrate the effectiveness of the proposed method. The influence of various design parameters on the strip shape is discussed. In comparison with previous research that employed triangles in the strip design, this work offers better surface developability, simpler solution for quick implementation, and more design handles for the shape control. It serves as a simple but practical method for CAGD of developable strip.

2. Preliminaries

2.1. Developable Bézier patch

Given two curves $\mathbf{P}(u)$ and $\mathbf{Q}(u)$ in 3D space, a ruled surface is constructed by linking each pair of corresponding curve points (with equal u) with a line segment $\mathbf{PQ}$, referred to as a ruling. The surface $\mathbf{R}$ is described as

$$\mathbf{R}(t,u) = (1-t)\,\mathbf{P}(u) + t\,\mathbf{Q}(u), \quad (t,u) \in [0,1] \times [0,1] \tag{1}$$

where t is the parameter along the ruling. Generally the tangent lines to the curves $\mathbf{P}(u)$ and $\mathbf{Q}(u)$ at any given point do not lie in the same plane. If these tangent lines and the corresponding ruling remain coplanar, then the surface becomes developable, which can be represented in terms of the triple scalar product of the two tangent vectors and the ruling vector $\mathbf{P}(u) - \mathbf{Q}(u)$ [9]:

$$\dot{\mathbf{P}}(u) \times \dot{\mathbf{Q}}(u) \cdot [\mathbf{P}(u) - \mathbf{Q}(u)] = 0 \tag{2}$$

Substituting the freeform representation of both curves into Eq. (2) leads to a complex system of equations that must be imposed on the control points to ensure the surface developability.

Imposing proper geometric restrictions on a patch can sometimes simplify the developability constraints and the solution process of the constrained control points. Several previous studies [6,7,10] applied this technique to make the surface design solvable. The resultant patches are special cases of the most general developable patch. Certainly these pre-defined limitations consume some degrees of freedom in the patch design, and thus reduce the modeling capability of the surface. For a developable Bézier patch, when the extensions of all the trapezoids in the Bézier control polyhedron intersect at a point $\mathbf{O}$ (see Fig. 1) and vectors $\mathbf{c}_0$, $\mathbf{c}_1$, and $\mathbf{c}_2$ in the patch must satisfy [9]:

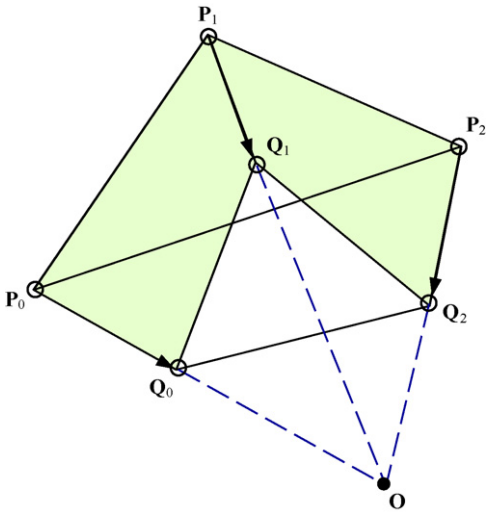

Fig. 1. A quadratic Bézier patch in generalized conical form.

$$\frac{\mathbf{c}_0}{\mathbf{P}_0\mathbf{O}} = \frac{\mathbf{c}_1}{\mathbf{P}_1\mathbf{O}} = \frac{\mathbf{c}_2}{\mathbf{P}_2\mathbf{O}} = f \tag{3}$$

where f and $\mathbf{O}$ are referred to as the scaling factor and the projection point, respectively. The patch becomes developable and refers to as the generalized conical form [9]. Eq. (3) indicates that one boundary curve is simply a scaled copy of the other curve. This conclusion also reveals that any control point pairs must remain coplanar. Any Bézier ruled patch with one boundary reduced into a single point is a triangular developable patch [28]. That is, any surface constructed by linking from a projection point to a Bézier curve becomes developable. Despite its limited modeling capability, the conical model provides simple but useful design methods in many applications of developable patches.

3. Modeling with developable Bézier patch

A strip is defined by two boundary curves. They are defined by piecewise parametric curves interpolating a set of sample points. The strip design in this work is to find a series of developable surfaces that interpolate the two curves. Assume they are denoted as $\mathbf{P}(u)$ and $\mathbf{Q}(u)$, the first step is to take a set of points $P = \{\mathbf{p}_1, \mathbf{p}_2, \ldots, \mathbf{p}_n\}$ and $Q = \{\mathbf{q}_1, \mathbf{q}_2, \ldots, \mathbf{q}_m\}$. To interpolate P and Q with maximal developability is a variation optimization problem [24]. This paper proposes a different approach which does not need to solve such a complex problem. The idea is to use developable patches to interpolate P and Q so that the developability is automatically preserved. At any ruling $\mathbf{p}_i\mathbf{q}_j$, we can choose two different elements to start with: a triangular or a quadrilateral developable patch. The following algorithms describe how to calculate the control points in each case.

3.1. Generation of a triangular patch

As described above, a triangular developable Bézier patch is defined with a projection point and a Bézier boundary curve. We choose the projection point and the end control points of the curve from the point sets P and Q. A curve constructed in this way would be of close proximity to the boundaries. As shown in Fig. 2, suppose $\mathbf{p}_i$ and $\mathbf{p}_{i+1}$ are two consecutive points in the set P, with the tangent vectors to the original curve denoted as $\mathbf{t}_i$ and $\mathbf{t}_{i+1}$. They serve as the

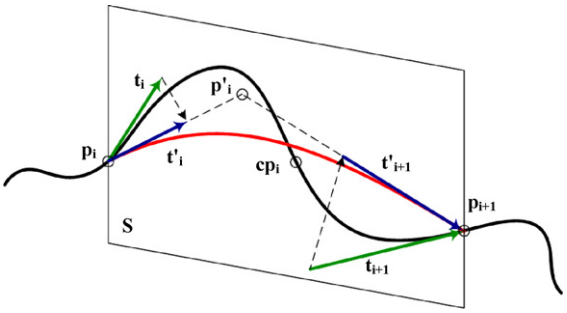

Fig. 2. Generation of the control polyhedron for a triangular developable Bézier patch.

end control points of a quadratic Bézier curve. The second control point can be determined in two different ways. The first possibility is the intersection between the tangent lines corresponding to $\mathbf{t}_i$ and $\mathbf{t}_{i+1}$. If they do not intersect, which is usually the case, then the solution is computed in a more complex manner. The middle point over the curve segment $\mathbf{p}_i\mathbf{p}_{i+1}$ (denoted as $\mathbf{cp}_i$), $\mathbf{p}_i$, and $\mathbf{p}_{i+1}$ determine a plane **S**. Let the tangent lines project into the plane, forming $\mathbf{t}'_i$ and $\mathbf{t}'_{i+1}$. Their intersection becomes the second control point. Note that the projection point is selected from the other boundary ($\mathbf{Q}(u)$ in this case). The choice of the control point is a heuristic rule and may not be an optimal solution. However, it gives satisfactory solutions in the test cases shown later.

3.2. Generation of a quadrilateral patch

Given four points on the strip boundaries, the corresponding boundary curve segments are denoted as $\mathbf{p}_i\mathbf{q}_i$ and $\mathbf{p}_{i+1}\mathbf{q}_{i+1}$, as shown in Fig. 3. Since these points are constructed in Step 2 of the above algorithm, they are coplanar—thus $\mathbf{p}_i\mathbf{q}_i$ and $\mathbf{p}_{i+1}\mathbf{q}_{i+1}$ intersect at the projection point **O**. Recall that the control polygon of one boundary must be a scaled copy of the other in the conical form. Thus only three control points among $\mathbf{p}_i$, $\mathbf{q}_i$, $\mathbf{p}_{i+1}$, and $\mathbf{q}_{i+1}$ can be freely specified once the projection point has been chosen. The end ruling may intersect the boundary at a different point $\mathbf{q}'_{i+1}$ from $\mathbf{q}_{i+1}$, given that $\mathbf{p}_i$, $\mathbf{q}_i$, and $\mathbf{p}_{i+1}$ as the chosen control points. The second control point $\mathbf{mp}_i$ of the longer curve segment is calculated from $\mathbf{p}_i$ and $\mathbf{p}_{i+1}$ using the same heuristic adopted in generation of a triangular patch. Once it has been obtained, the remaining control point $\mathbf{mq}_i$ of the shorter segment is then determined by Eq. (3).

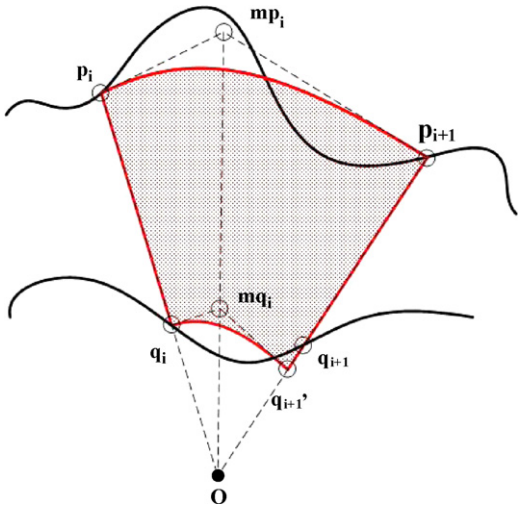

Fig. 3. Generation of the control polyhedron for a quadrilateral developable Bézier patch.

3.3. Algorithm for generation of developable patches in the conical form

Step 1: generate point sets from the boundary curves.

This step divides the given boundary curves into two point sets with equal arc length. The number of points in *P* and *Q* does not have to be equal.

Step 2: test feasibility of constructing a quadrilateral patch.

The proposed method adopts a heuristic in the strip design, i.e., we prefer use of a quadrilateral patch, following the same idea, this step checks whether a quadrilateral patch can be constructed in the first place, even though a triangular one always exists. Fig. 4(a) shows that $\mathbf{p}_i\mathbf{q}_j$ is a ruling to start with. The tangent vectors to the curves at these points are $\mathbf{tp}_i$ and $\mathbf{tq}_j$. If they lie on the same side of the triangle $\mathbf{p}_i\mathbf{p}_{i+1}\mathbf{q}_j$, then go to Step 3 for testing other conditions that must be satisfied in construction of a developable patch. The similar test is carried out when both vectors remain on one side of the triangle $\mathbf{p}_i\mathbf{q}_j\mathbf{q}_{j+1}$. A triangular patch will be considered only when those vectors are located on different sides of the two triangles.

Step 3: test the construction feasibility of a developable patch.

Given a ruling $\mathbf{p}_i\mathbf{q}_j$, there are four different ways in constructing the next patch. First, we can choose a triangular or a quadrilateral patch. The projection point of each patch is likely to be located on either curve. The potential solutions are referred to as candidate patches in this paper. Their corresponding construction procedures are described as follows:

(1) Quadrilateral patch $\mathbf{p}_i\mathbf{p}_{i+1}\mathbf{q}_j$: we calculate the intersection between the plane determined by $\mathbf{p}_i$, $\mathbf{p}_{i+1}$, and $\mathbf{q}_j$ and the boundary curve **Q**. The one nearest to $\mathbf{q}_j$ (denoted as $\mathbf{q}'_j$) is chosen when there are multiple solutions, as shown in Fig. 4(b). If the distance between $\mathbf{q}'_j$ and $\mathbf{q}_j$ is smaller than the Hausdorff distance specified by the user, then $\mathbf{p}_i$, $\mathbf{p}_{i+1}$, and $\mathbf{q}_j$ allow the construction of a quadrilateral developable patch. These points cannot form a quadrilateral developable patch when there is no intersection or the limitation of the distance is not satisfied.

(2) Quadrilateral patch $\mathbf{p}_i\mathbf{q}_j\mathbf{q}_{i+1}$: we calculate the intersection between the plane determined by $\mathbf{p}_i$, $\mathbf{q}_i$, and $\mathbf{q}_{j+1}$ and the boundary curve **P**. The one nearest to $\mathbf{p}_j$ (denoted as $\mathbf{p}'_j$) is chosen when there are multiple solutions, as shown in Fig. 4(d). If the distance between $\mathbf{p}'_j$ and $\mathbf{p}_j$ is smaller than the Hausdorff distance specified by the user, then $\mathbf{p}_i$, $\mathbf{q}_i$, and $\mathbf{q}_{j+1}$ allow the construction of a quadrilateral developable patch.

(3) Triangular patch $\mathbf{p}_i\mathbf{q}_j\mathbf{q}_{i+1}$: the next point $\mathbf{q}_{i+1}$ on **Q** is chosen to form a triangular developable patch along with the ruling $\mathbf{p}_i\mathbf{q}_j$, as shown in Fig. 4(f), with $\mathbf{p}_i$ as the projection point. It is necessary to check the distance between $\mathbf{p}_i$ and $\mathbf{q}_{i+1}$ with respect to the Hausdorff distance.

(4) Triangular patch $\mathbf{p}_i\mathbf{p}_{i+1}\mathbf{q}_j$: the next point $\mathbf{p}_{i+1}$ on **P** is chosen to form a triangular developable patch along with the ruling $\mathbf{p}_i\mathbf{q}_j$, as shown in Fig. 4(g), with $\mathbf{q}_i$ as the projection point.

Step 4: choose an optimal solution from the candidate patches.

Step 3 may generate multiple solutions starting with $\mathbf{p}_i\mathbf{q}_j$. Since a quadrilateral patch has higher preference, it surpasses both triangular patches. If there are two feasible quadrilateral patches (with the projection point on the different sides), they are evaluated using a given criterion. The one corresponding to a smaller value will be selected. The similar evaluation process is applied to choose between two triangular patches.

Step 5: repeat Steps 2 to 4 until the end ruling reaches $\mathbf{p}_m\mathbf{q}_n$.

4. Continuity adjustment with degree elevation

Any consecutive patches generated from the above algorithms only guarantee positional continuity across the patch boundary.

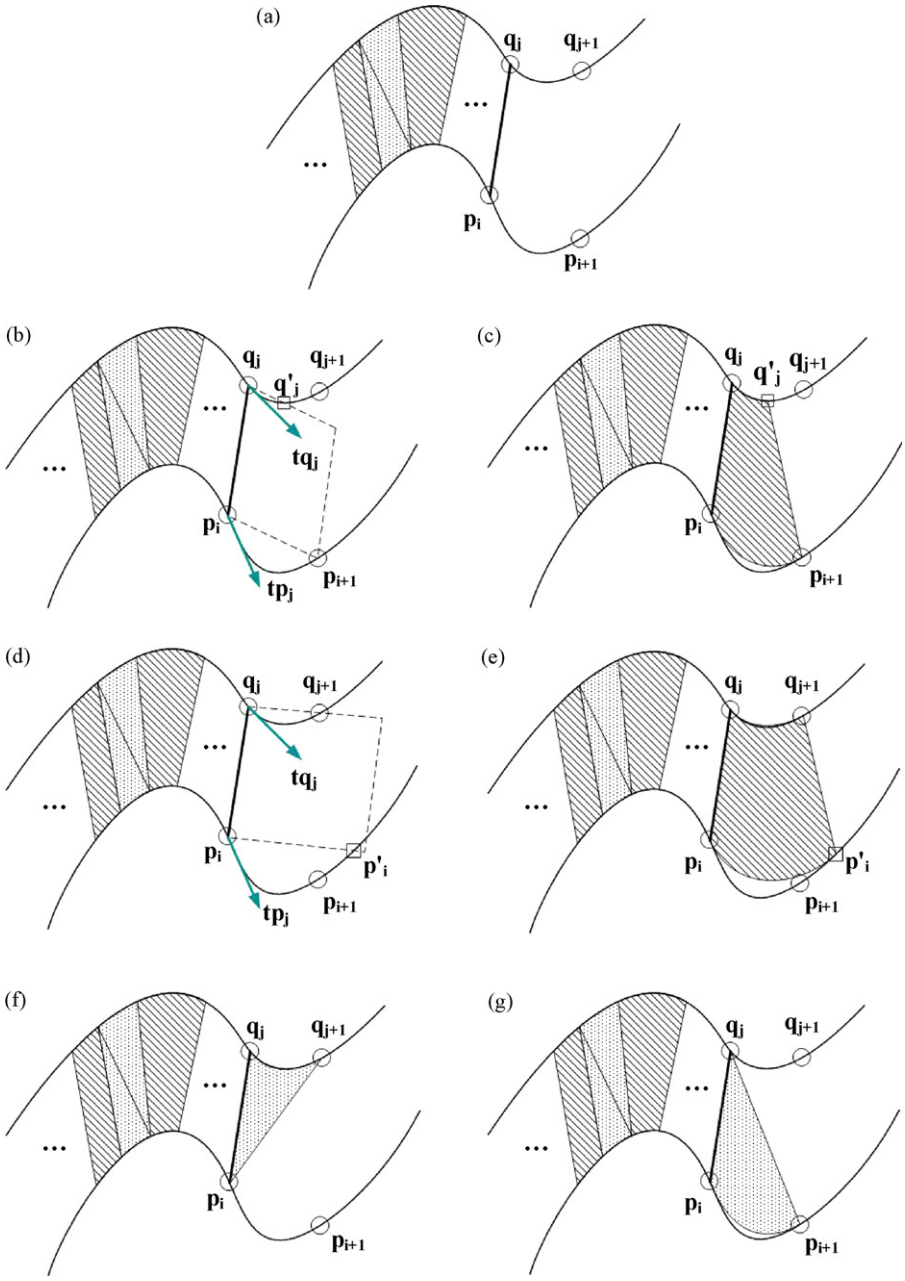

Fig. 4. Generation of a developable patch at a ruling.

This may restrict the practicality of the result in many occasions. Here we propose an effective technique to overcome this problem. The idea is to gain additional degrees of freedom for finer adjustment of a Bézier patch through degree elevation [11]. These extra design handles not only allow the continuity adjustment, but they can be also used to maintain the surface developability at the same time. The principle of degree elevation for a Bézier patch will be discussed as follows.

4.1. Degree elevation

Degree elevation increases the degree of a curve without changing the shape of the curve. This technique was originally developed for combining two curves of different degrees, thus simplifying the complexity of geometric processing. Given a n-degree Bézier curve with control points $\mathbf{P}_0$, $\mathbf{P}_1$, …, $\mathbf{P}_n$, the new control points $\mathbf{p}'_i$ for the Bézier curve of degree $(n+1)$ can be written as [29]:

$$\begin{aligned} &\mathbf{p}'_0 = \mathbf{p}_0, \qquad \mathbf{p}'_{n+1} = \mathbf{p}_n \\ &\mathbf{p}'_i = \frac{i}{n+1}\mathbf{p}_{i-1} + \left(1 - \frac{i}{n+1}\right)\mathbf{p}_i, \quad i = 1, 2, \ldots, n \end{aligned} \tag{4}$$

For a quadratic Bézier ruled surface with $\mathbf{A}_0$–$\mathbf{A}_1$–$\mathbf{A}_2$ and $\mathbf{B}_0$–$\mathbf{B}_1$–$\mathbf{B}_2$ as the control points of its boundary curves (see Fig. 5), the new control points for the same surface of degree three become:

$$\begin{aligned} &\mathbf{A}'_0 = \mathbf{A}_0, \quad \mathbf{A}'_4 = \mathbf{A}_3, \quad \mathbf{B}'_0 = \mathbf{B}_0, \quad \mathbf{B}'_4 = \mathbf{B}_3 \\ &\mathbf{A}'_1 = \frac{1}{3}\mathbf{A}_0 + \frac{2}{3}\mathbf{A}_1, \quad \mathbf{A}'_2 = \frac{2}{3}\mathbf{A}_1 + \frac{1}{3}\mathbf{A}_2, \quad \mathbf{B}'_1 = \frac{1}{3}\mathbf{B}_0 + \frac{2}{3}\mathbf{B}_1, \\ &\mathbf{B}'_2 = \frac{2}{3}\mathbf{B}_1 + \frac{1}{3}\mathbf{B}_2 \end{aligned} \tag{5}$$

A patch degree-elevated from a patch of a lower degree still preserves the developability of the surface, since the elevation process only changes the parameterization of the surface, not its

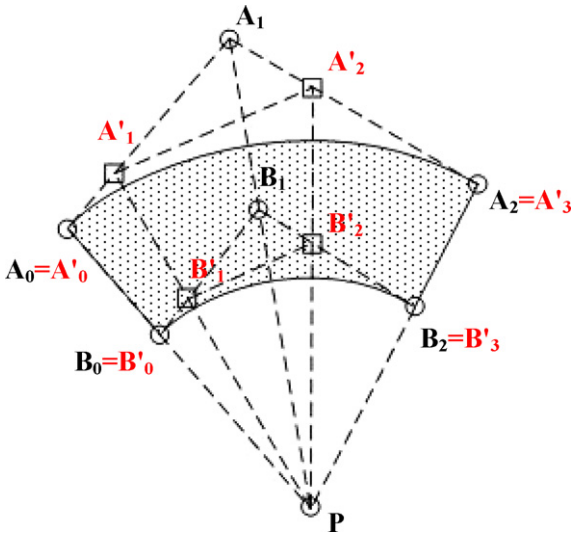

Fig. 5. Degree elevation for a quadratic Bézier ruled surface.

shape. For a patch in the conical form, the projection point remains the same and each control point pair satisfies the scaled relationship. On the other hand, there are more design handles in the new representation of the surface that can be utilized to modify the control points with finer shape control. The next section will introduce a set of algorithms that generate G1 continuity across the patch boundaries based on this idea.

4.2. Algorithms for continuity adjustment with degree elevation

4.2.1. Continuity adjustment for quadrilateral patch

Fig. 6 shows the control points of a quadrilateral patch involved in the adjustment process. Initially, the patch $\mathbf{S}_i$ connects to $\mathbf{S}_{i-1}$ and $\mathbf{S}_{i+1}$ along the rulings $\mathbf{A}_0\mathbf{B}_0$ and $\mathbf{A}_3\mathbf{B}_3$, respectively, both with positional continuity. For $\mathbf{S}_{i-1}$, the tangent vectors to the boundary curves at $\mathbf{A}_0$ and $\mathbf{B}_0$ are $\mathbf{t}_\mathbf{A}$ and $\mathbf{t}_\mathbf{B}$, which has been determined when processing the patch $\mathbf{S}_{i-1}$ (i.e., they are fixed and coplanar—when $\mathbf{S}_i$ is a starting patch, we simply assign the average of $\mathbf{t}_\mathbf{A}$ and $\mathbf{t}_\mathbf{B}$ as the strip tangent). To achieve G1 across $\mathbf{A}_0\mathbf{B}_0$, we must let (1) $\mathbf{A}_1$ lies in the direction of $\mathbf{t}_\mathbf{A}$, and (2) $\mathbf{B}_1$ lies in the direction of $\mathbf{t}_\mathbf{B}$.

To achieve G1 across $\mathbf{A}_3\mathbf{B}_3$ is slightly tricky. Instead of the original control polygon, a scaled copy (denoted as $\mathbf{A}'_0 - \mathbf{A}'_1 - \mathbf{A}'_2 - \mathbf{A}'_3$) contains the last control point $\mathbf{A}'_3$ located on the boundary. We have $\mathbf{A}_2\mathbf{A}_3 // \mathbf{A}'_2\mathbf{A}'_3$ in the conical form. Thus, G1 requires (1) $\mathbf{A}_2$ (or $\mathbf{A}'_2$) lies in the direction of $\mathbf{t}'_\mathbf{A}$, and (2) $\mathbf{B}_2$ lies in the direction of $\mathbf{t}'_\mathbf{B}$. To determine the control points on $\mathbf{S}_{i+1}$, $\mathbf{t}'_\mathbf{A}$ and $\mathbf{t}'_\mathbf{B}$ are chosen as the average of the original tangent vectors on the boundary curves at $\mathbf{A}_3$ (or $\mathbf{A}'_3$) and $\mathbf{B}_3$. Then, we have $\mathbf{A}_1 = \mathbf{A}_0 + w_1\mathbf{t}_\mathbf{A}$ and $\mathbf{A}_2 = \mathbf{A}_3 - w_2\mathbf{t}'_\mathbf{A}$. They also specify the positions of $\mathbf{B}_1$ and $\mathbf{B}_2$. After preserving the G1 continuity and the developability, we still have 2-DOF for further adjustment of the shape of $\mathbf{S}_i$, i.e., w_1 and w_2. $\mathbf{t}'_\mathbf{A}$ and $\mathbf{t}'_\mathbf{B}$ act as the starting tangent vectors for the next patch $\mathbf{S}_{i+1}$. Note that all tangent vectors are normalized.

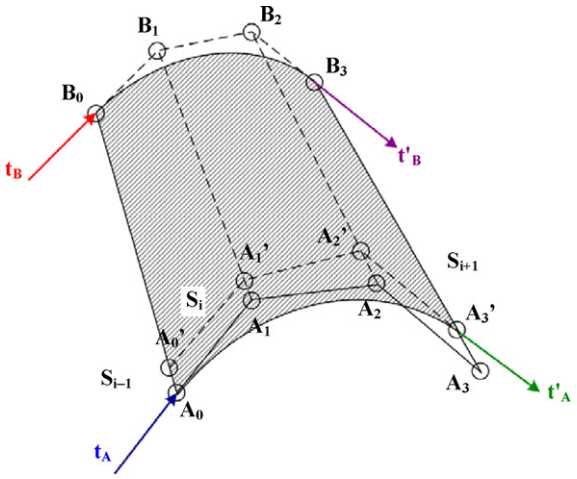

Fig. 6. Continuity adjustment for a quadrilateral patch.

4.2.2. Continuity adjustment for triangular patch

When processing a triangular patch $\mathbf{S}_i$, the situation becomes more complex than the quadrilateral patch—we need to analyze the possible configurations on the next patch $\mathbf{S}_{i+1}$. As shown in Fig. 7, if only considering about the developability on the triangular patch $\mathbf{S}_i$, the tangent vectors $\mathbf{t}_\mathbf{A}$, $\mathbf{t}_\mathbf{B}$, $\mathbf{t}'_\mathbf{A}$ and $\mathbf{t}'_\mathbf{B}$ do not have to be coplanar. However, we need to take into account the developability constraints imposed by the next patch $\mathbf{S}_{i+1}$ at the same time when choosing them. In detail,

- When $\mathbf{S}_{i+1}$ is a quadrilateral patch, we must have $\mathbf{t}'_\mathbf{A} // \mathbf{t}'_\mathbf{B}$ so that $\mathbf{S}_{i+1}$ becomes developable. Meanwhile, we need to have $\mathbf{t}_\mathbf{B} // \mathbf{t}'_\mathbf{B}$ so that the G1 continuity is preserved at $\mathbf{B}_0$. Therefore, in this configuration, the tangent vectors on the end ruling must satisfy $\mathbf{t}'_\mathbf{B} // \mathbf{t}_\mathbf{B}$ and $\mathbf{t}'_\mathbf{A} // \mathbf{t}'_\mathbf{B}$.
- When $\mathbf{S}_{i+1}$ is a triangular patch with the projection point at $\mathbf{B}_0$ (or $\mathbf{A}_3$), we give $\mathbf{t}_\mathbf{B} // \mathbf{t}'_\mathbf{B}$ so that the G1 continuity is given at $\mathbf{B}_0$. Then, $\mathbf{t}'_\mathbf{A}$ is assigned to follow the boundary curve tangent of the strip at $\mathbf{A}_3$.

After determining the directions of the tangent vector on the start and end rulings of $\mathbf{S}_i$, the control points $\mathbf{A}_1$ and $\mathbf{A}_2$ can be computed by $\mathbf{A}_1 = \mathbf{A}_0 + w_1\mathbf{t}_\mathbf{A}$ and $\mathbf{A}_2 = \mathbf{A}_3 - w_2\mathbf{t}'_\mathbf{A}$. In this case, we still have 2-DOF to adjust the shape of $\mathbf{S}_i$ after preserving G1 and developability.

5. Implementation results

5.1. Surface evaluation criteria

Given a pair of spatial curves, different strips can be generated and all interpolate the same curves. They should be accessed

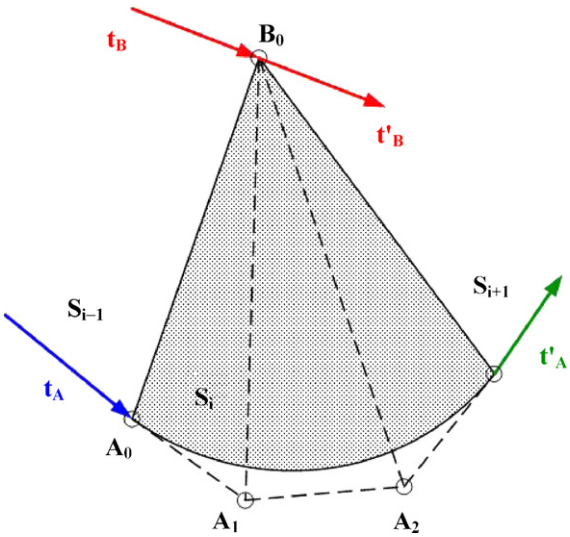

Fig. 7. Continuity adjustment for a triangular patch.

quantitatively based on some criteria depending on specific applications. These criteria also work as optimization objectives in the design of the geometric design algorithms. A simple objective is minimal area [30], i.e., the resultant patch set has the minimal surface area among all the solutions. Other optimization objectives include maximal developability, minimal bending energy, and minimal normal variation. This paper will adopt normal variation and bending energy as the major objectives to be minimized in the design process.

Fig. 8 illustrates two consecutive patches connecting along the ruling $\mathbf{p}_i\mathbf{q}_j$. Since both patches are in the conical form, any two pairs of the control points must be co-planar. The corresponding normal vectors of $\mathbf{S}_k$ and $\mathbf{S}_{k+1}$ at the ruling are $\mathbf{n}_k$ and $\mathbf{n}_{k+1}$, respectively. The normal variation (or normal twist) across $\mathbf{p}_i\mathbf{q}_j$ can be expressed as

$$N_v(\mathbf{S}_k, \mathbf{S}_{k+1}) = 1 - \mathbf{n}_k \cdot \mathbf{n}_{k+1} \tag{6}$$

It becomes null when the two vectors are in the same directions. The total normal variation of the approximation result consisting of M patches becomes:

$$N_T(M) = \sum_{k=0}^{M-1} N_v(\mathbf{S}_k, \mathbf{S}_{k+1}) \tag{7}$$

Note that the calculation of the normal variation is regardless of the patch type (triangular or quadrilateral).

Energy was considered a good objective for functional optimization of surface fairness [31] in that it gives an integral measure of the surface curvature. This study employs bending energy as one objective to be minimized, which can be simplified into the following form along a ruling shared by two successive

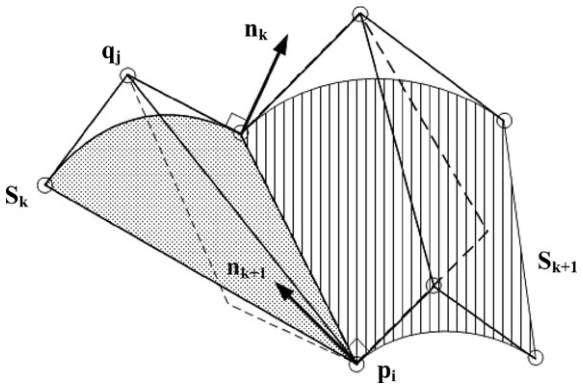

Fig. 8. Calculation of normal variation across two consecutive patches.

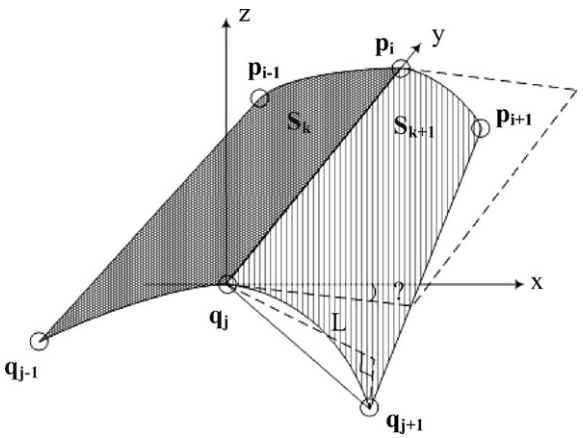

Fig. 9. Calculation of bending energy across two consecutive patches.

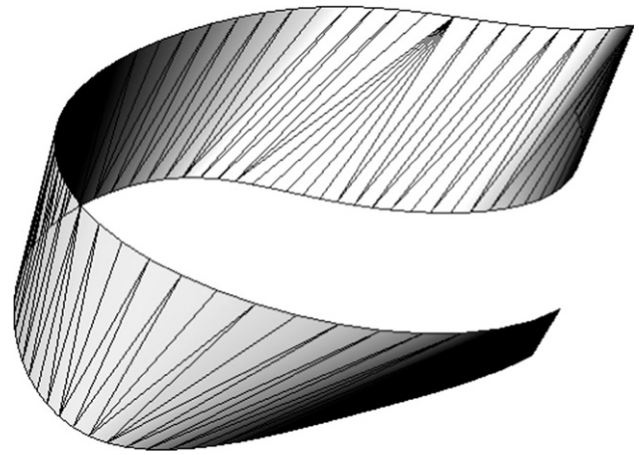

Fig. 10. The first test result of the BBT method [24].

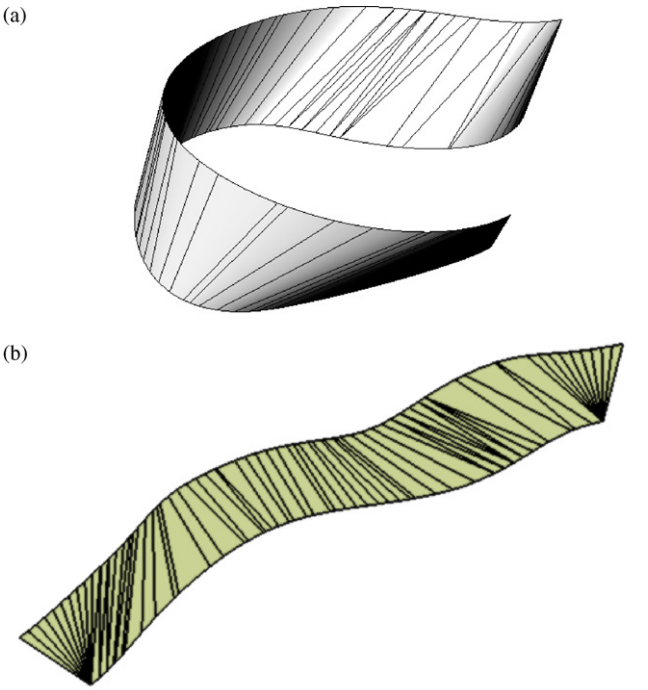

Input Parameter						Current Method			BBT Method
O_L	N_p	N_q	H_3	H_4	r_a	n_3	n_4	N_T	N_T
NT	55	65	4	4	1.2	33	39	0.128747	5.3

Fig. 11. The first test result based on optimization of normal variation.

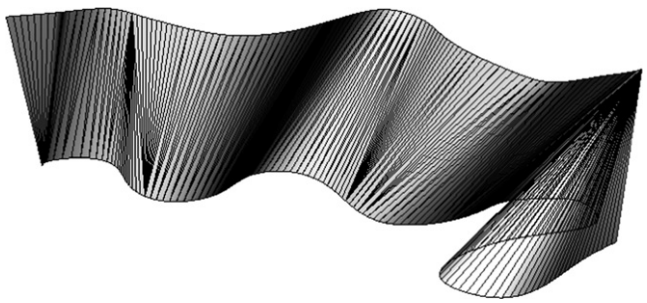

Fig. 12. The second test result of the BBT method [24].

patches at a small bending angle:

$$U_k = K\frac{A\sin^2\theta}{L^2} \tag{8}$$

where K is a coefficient determined by the thickness of surface and the Young's modulus [22]. As shown in Fig. 9, L is the moment arm of the patch $\mathbf{S}_k$ with respect to the rotation axis $\mathbf{p}_i\mathbf{q}_j$. It is computed as the maximal perpendicular distance from the patch to the axis. θ is the angle extended by the tangent planes of $\mathbf{S}_k$ and $\mathbf{S}_{k+1}$ at the ruling. A is the surface area of $\mathbf{S}_{k+1}$. K is set to one for simplification purpose. The total bending energy containing in an aggregate of M developable patches can be written as

$$U_B(M) = \sum_{k=0}^{M-1} U_k \tag{9}$$

5.2. Test results

This section presents a number of examples to validate the feasibility of the proposed method. Different input parameters are examined to characterize their individual effects on the design result. The same boundary curves employed by the previous work [24] are used for comparison. The input parameters include the optimization objective (O_L), the numbers of sample point on the boundaries (N_p/N_q), the Hausdorff distance for triangular (H_3) and quadrilateral patches (H_4), and the maximal length ratio between the boundaries of quadrilateral patch (r_a). The output properties include the surface evaluation value, the number of triangular

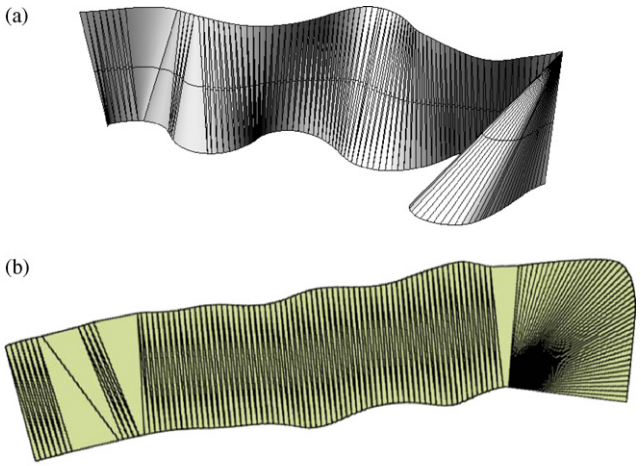

Input Parameter						Current Method			BBT Method
O_L	N_p	N_q	H_3	H_4	r_a	n_3	n_4	U_B	U_B*
BE	144	91	4	10	1.5	200	14	70.5874	77.0

Fig. 13. The second test example based on optimization of bending energy.

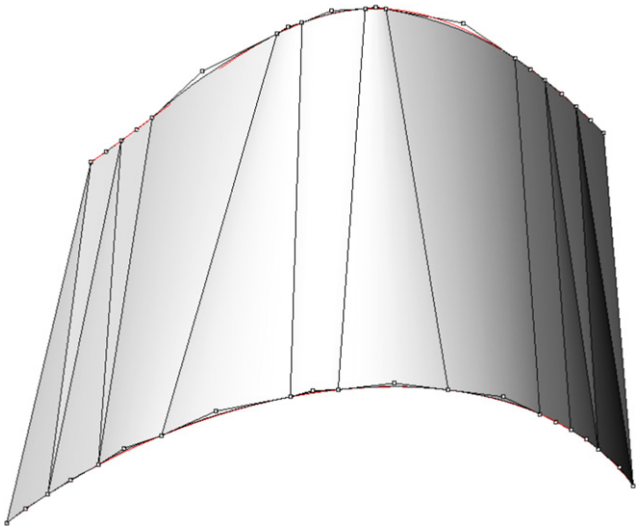

Fig. 14. Strip design with two input curves with less twist.

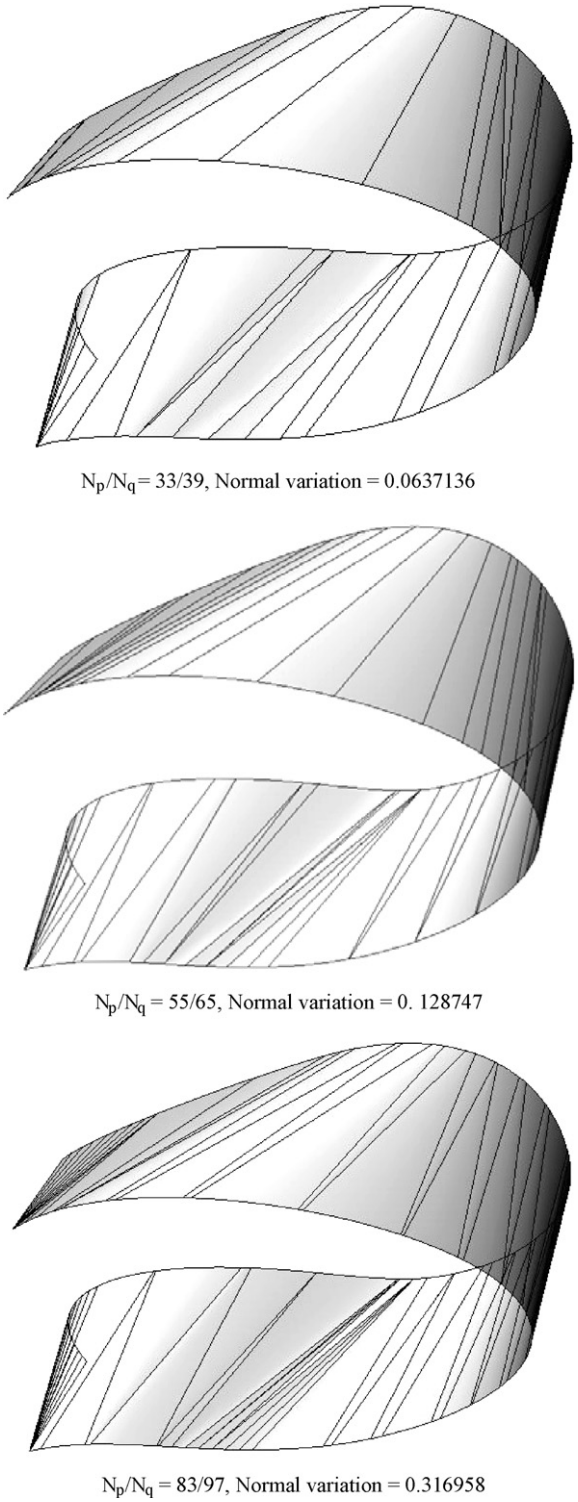

Fig. 15. Approximation results with different N_p/N_q values.

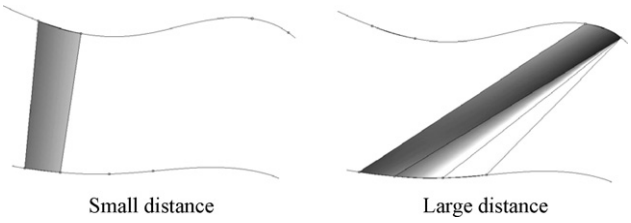

Fig. 16. Large Hausdorff distances produce skew quadrilateral patches.

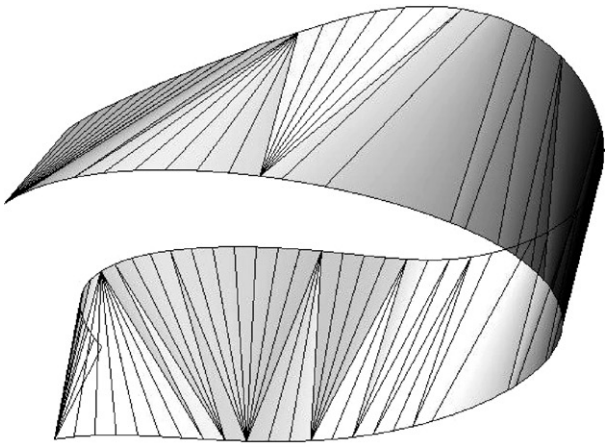

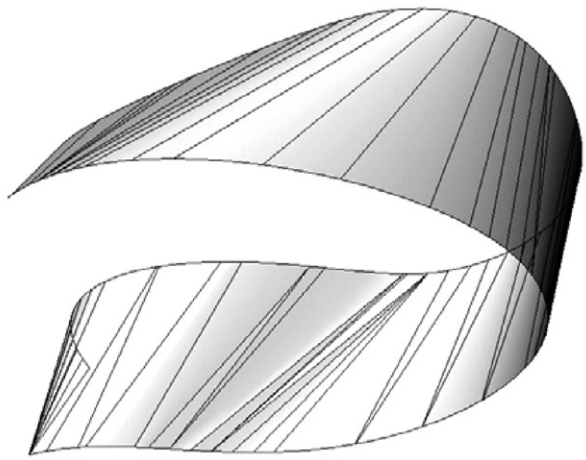

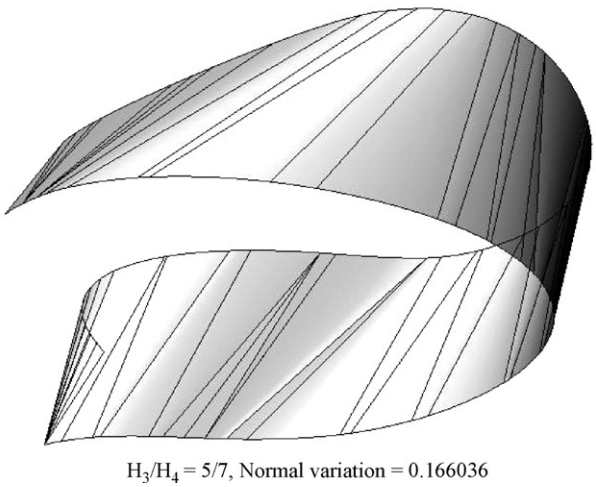

Fig. 17. Approximation results with different H_3/H_4 values.

patches n_3, and the number of quadrilateral patches n_4. NT and BE denote "normal variation" and "bending energy", respectively, in the results.

Note that each triangle shown in the following figures represents a Bezier patch of the final surface. Fig. 10 illustrates the result from the previous work using the BBT method [24]. Fig. 11 shows the strip design generated from our method with the same parameters except r_a, which the past work does not offer. Fig. 11(a) demonstrates the strip consisting of 33 triangular and 39 quadrilateral patches. Fig. 11(b) shows the unfolded pattern from the patches. Our method outperforms the BBT method in terms of the normal variation. The second strip consists of two highly convoluted curves. Fig. 12 is the result generated by the BBT method. Fig. 13 shows the strip generated by our method based on optimization of bending energy. It contains only four quadrilateral patches, as the curvature varies radically along the curves. The distribution of the triangular patches is different from the one in Fig. 12. The current method gives a slightly better result in terms of bending variation. However, the BBT method computes one energy value from two consecutive triangles in an approximate manner, whereas the current method computes the value from continuous integral of every single patch.

Fig. 14 shows the test result of two boundary curves with relatively less twist. The objective is to minimize the normal twist. The strip consists of six quadrilateral patches and eight triangular ones. The control points of these patches are also illustrated in the figure. The following sections will highlight the test results with different input parameters. The focus is to illustrate how individual parameters affect the strip, the composition of triangular and quadrilateral patches, and the evaluation values of the approximation result. We also try to provide useful insights to how each parameter changes the final shape. All the examples interpolate the two curves in the first test example with the same input parameters as those in Fig. 10, except the one that is being investigated in each case.

5.3. Numbers of sample points

Sample points with equal arc length are taken from the two boundary curves. Each curve may have different numbers of points due to their length difference. Fig. 15 demonstrates the corresponding patch sets under different test conditions. The results are examined from several aspects. First, the evaluation values increase with the number of the sample points. A possible reason is that more patches are generated (notice the successive triangular patches are increased), and the variation of the surface

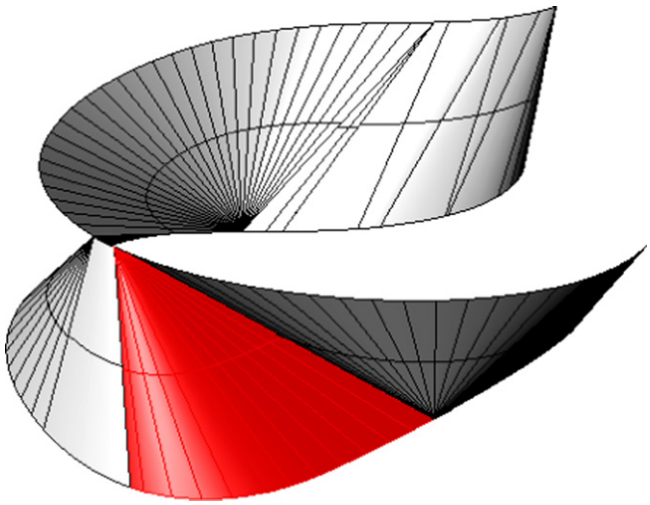

Fig. 18. More consecutive triangular patches are produced with a larger H_3 value.

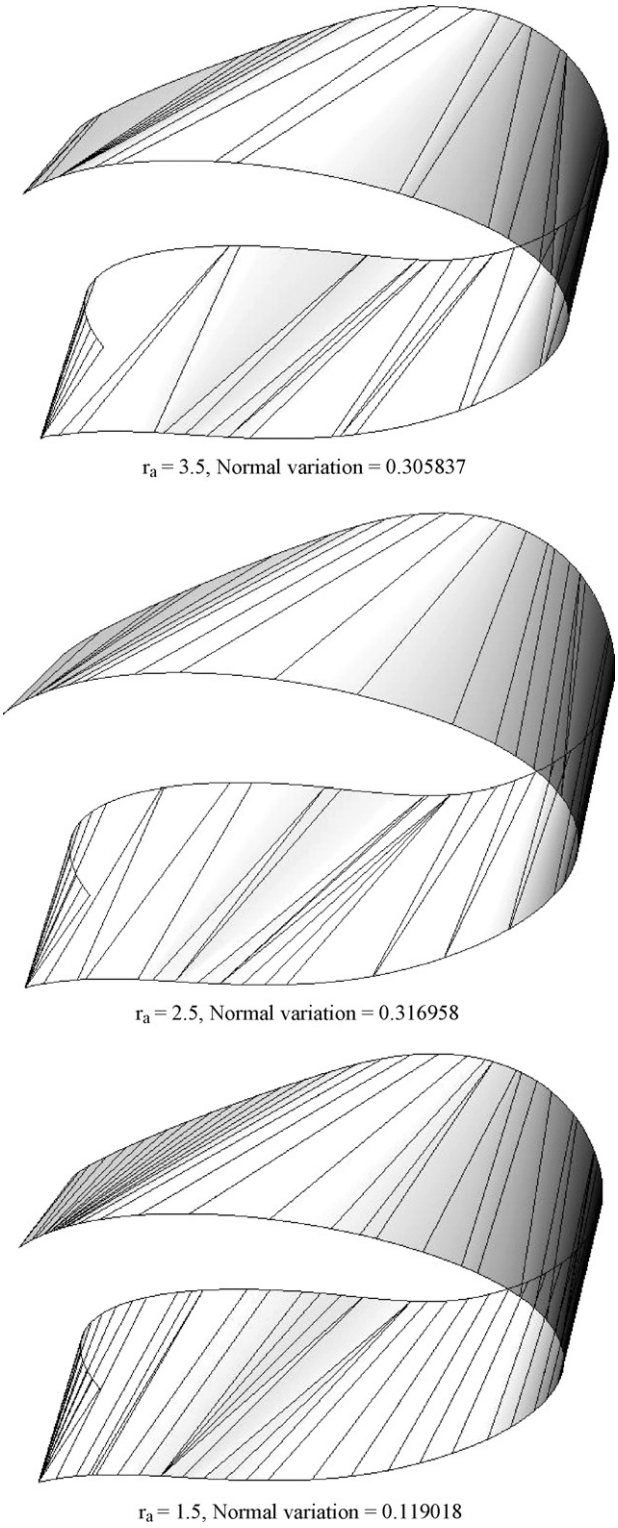

Fig. 19. Approximation results with different r_a values.

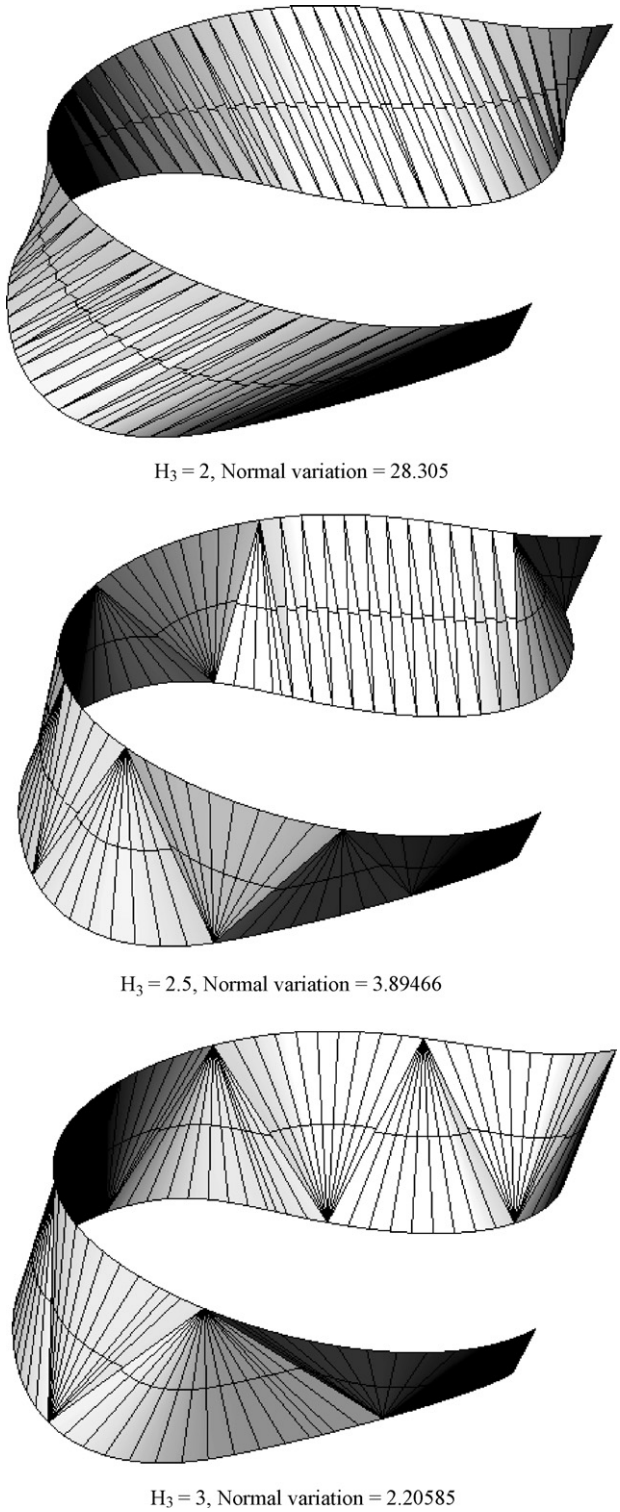

Fig. 20. Approximation results with different limitations on the triangular patch size.

normal only occurs at the patch boundary. On the other hand, the deviation of the strip design from the boundaries becomes evident when the point numbers are too small.

5.4. Hausdorff distances

Hausdorff distances have a distinct influence on the composition of triangular/quadrilateral patches in the design result. They control generation of the candidate patches by limiting the sizes of triangular and quadrilateral patches. The distance for triangular patch restricts the number of consecutive patches with the same projection point. The maximal edge length of triangular patch is reduced when the projection point is alternating. The distance also determines the skewness of the feasible quadrilateral patches as shown in Fig. 16. The distribution of triangular and quadrilateral patches varies as these distances change, which corresponds to

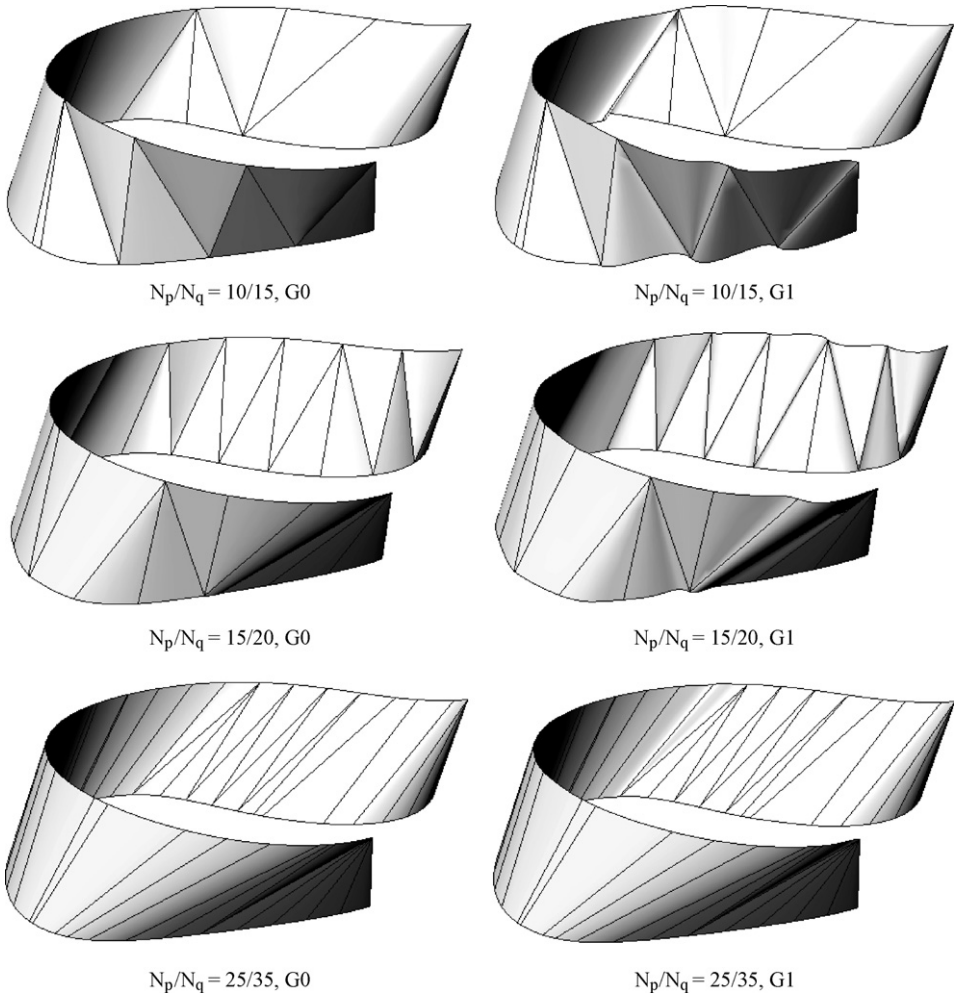

Fig. 21. G0 and G1 approximation results with different numbers of sample points.

different shapes, appearances, and evaluation values of the strip. Fig. 17 illustrates the patch sets corresponding to different Hausdorff distances. The effect of these distances is somewhat complicated. Large H_3 usually produces more consecutive triangular patches with the same projection point. The surface normal has an excessive jump across the last ruling of the consecutive patches, at which either the projection point switches to the other side (see Fig. 18) or a quadrilateral patch is connected. Quadrilateral patch is more likely to occur at large H_4, but the deviation from the boundaries is also increased.

5.5. Maximal length ratio of the boundaries in quadrilateral patch

This parameter limits the length difference between the boundaries of a quadrilateral patch. It has a compound effect on the strip design. A large value may allow generation of a quadrilateral patch with the similar effect on the evaluation criteria as a large number of consecutive triangular patches. Under this circumstance, the construction process of the surface may have fallen into a local optimum due to the selection process (see Step 4 in *Algorithm for generation of developable patches in the conical form*). Such a patch could be a better choice in the local region of concern, but it certainly does not lead to a global optimum. "Normal" quadrilateral patches are more likely to occur when the ratio is small. They usually give more satisfying surfaces, as shown in Fig. 19.

The strip will consist of only triangular patches by proper combination of the input parameters. Fig. 20 shows such examples with small H_4 values. This condition always makes quadrilateral patches infeasible in the surface construction process. The result containing only triangular patches, especially with large H_3, usually has a larger evaluation value than the one properly made of both triangular and quadrilateral patches. Another notable observation is that the larger the proportion of quadrilateral patches in the patch set, the smaller the objective function is.

Fig. 21 illustrates different test results after continuity adjustment. According to Eqs. (7) and (9), both normal variation and bending energy vanish across the boundary of two consecutive developable patches with G1. The wrinkle effect becomes more evident in the modified patches. They provide better modeling capability of special effects like creases and folds compared to the result that is only G0, especially when the number of sample points is small. However, the deviation from the original boundaries becomes more distinct. This discrepancy is less evident with more sample points (see the result with N_p/N_q = 25/35 in the figure). It is probably true that no approximation methods can produce good results with the sample points less than a certain degree.

6. Conclusions and future work

This paper presents a CAGD method that interpolates a strip specified by two space curves with developable patches in the

conical form. The first step of the method calculates feasible patches that connect to a given ruling defined by two points on each curve. A heuristic is applied to select a local optimal solution in terms of a surface assessment criterion. The constructed strip consists of consecutive developable patches, triangular or quadrilateral, with positional continuity across the patch boundaries. Degree elevation is then conducted to produce extra degrees of freedom. We propose geometric algorithms that produce G1 continuity across the patches and preserve the developability of the surfaces at the same time, by adjusting the control points of the degree-elevated patches with these design parameters.

A variety of examples are generated using different input parameters. They demonstrate that our method outperforms the previous method that only used triangles in the strip design. We also discuss how each parameter influences the design result. The surface evaluation values increase with the numbers of sample points, as more patches are generated. The Hausdorff distances control the number of consecutive triangular patches and the skewness of quadrilateral patches. The ratio limitation of quadrilateral patch has a compound effect on how the surface is composed of triangular/quadrilateral patches. The large values usually cause increase of the assessment values. Only triangular patches are obtained with smaller Hausdorff distances for quadrilateral patch. Finally, the degree-elevated patches that have been adjusted with G1 offer more distinct modeling effects of wrinkle with fewer patches.

This work provides a simple but effective method for design of a strip using developable surfaces. In comparison with previous studies, it allows quicker implementation, better evaluation values of surface, and more flexible shape control of the design result. One major advantage is the ability of using triangular and quadrilateral patches simultaneously in the strip design. The former fits well in the highly convoluted areas whereas the latter approximates smooth regions with fewer patches. Another benefit is being able to perform local shape adjustment via degree elevation. A complete (or nearly) developable strip can be thus obtained. One major limitation of this work is that the result is not a global optimum (if it exists). A possible solution is to adopt some global optimization scheme (e.g. Genetics Algorithm) that computes the strip with the proposed methods in one iteration. A potential problem induced by our method is a larger amount of data storage compared with the design using triangles. Another limitation of this work is that a large number of patches are required to control the deviation from the input curves and to maintain G1 continuity at the same time in the strip. One solution is to recursively subdivides a small number of patches only when it is necessary. Finally, it is advantageous to fully utilize the extra degrees of freedom produced by degree elevation. They allow multiple objectives or complex objectives optimization in the strip design, which significantly enhance the practicality of developable strips in product realization.

References

[1] M.J. Mancewicz, W.H. Frey, Developable surfaces: properties, representations and methods of design, GM Research Publication GMR-7637, 1992.
[2] T. Lamb, Shell development computer aided lofting—is there a problem or not? Journal of Ship Production 11 (1) (1995) 34–46.
[3] T.J. Norlan, Computer aided design of developable surfaces, Marine Technology 8 (1971) 233–242.
[4] B.K. Hinds, J. McCartney, G. Woods, Pattern development for 3D surfaces, Computer-Aided Design 23 (8) (1991) 583–592.
[5] C.C.L. Wang, Y. Wang, M.M.F. Yuen, Design automation for customized apparel products, Computer-Aided Design 37 (7) (2005) 675–691.
[6] G. Aumann, Interpolation with developable Bézier patches, Computer-Aided Geometric Design 8 (1991) 409–420.
[7] J. Lang, O. Röschel, Developable $(1, n)$-Bézier surfaces, Computer-Aided Geometric Design 9 (1992) 291–298.
[8] T. Maekawa, J.S. Chalfant, Design and tessellation of B-spline developable surfaces, ASME Transaction Journal of Mechanical Design 120 (1998) 453–461.
[9] C.H. Chu, C.H. Séquin, Developable Bézier patches: properties and design, Computer-Aided Design 34 (7) (2002) 511–527.
[10] G. Aumann, A simple algorithm for designing developable Bézier surface, Computer-Aided Geometric Design 20 (2004) 601–616.
[11] G. Aumann, Degree elevation and developable Bézier surfaces, Computer-Aided Geometric Design 20 (2004) 661–670.
[12] H. Pottmann, J. Wallner, Computational Line Geometry, Springer–Verlag, 2001.
[13] R.M.C. Bodduluri, B. Ravani, Geometric design and fabrication of developable Bézier and B-spline surfaces, ASME Transactions Journal of Mechanical Design 116 (1994) 1024–1048.
[14] R.M.C. Bodduluri, B. Ravani, Design of developable surfaces using duality between plane and point geometry, Computer-Aided Design 25 (1995) 621–632.
[15] T. Randrup, Approximation of surfaces by cylinders, Computer-Aided Design 30 (1998) 807–812.
[16] S. Leopoldseder, H. Pottmann, Approximation of developable surfaces with cone spline surfaces, Computer-Aided Design 30 (1998) 571–582.
[17] H. Pottmann, T. Randrup, Rotational and helical surface approximation for reverse engineering, Computing 60 (1998) 307–323.
[18] H.Y. Chen, I.K. Lee, S. Leopoldseder, H. Pottmann, T. Randrup, J. Wallner, On surface approximation using developable surfaces, Graphical Models and Image Processing 61 (1999) 110–124.
[19] H. Pottmann, J. Wallner, Approximation algorithms for developable surfaces, Computer-Aided Geometric Design 16 (1999).
[20] C.C.L. Wang, Y. Wang, Y.F.M. Yuan, On increasing the developability of a trimmed NURBS surface, Engineering with Computers 20 (2004) 54–64.
[21] C.C.L. Wang, K. Tang, Achieving developability of a polygonal surface by minimum deformation: a study of global and local optimization approaches, The Visual Computer 20 (2004) 521–539.
[22] K. Tang, C.C.L. Wang, Modeling developable folds on a strip, Journal of Computing and Information Science in Engineering 5 (2005) 35–47.
[23] W.H. Frey, Boundary triangulations approximating developable surfaces that interpolate a closed space curve, Computer-Aided Design 13 (2) (2002) 285–302.
[24] K. Tang, C.C.L. Wang, Optimal boundary triangulations of an interpolating ruled surface, Journal of Computing and Information Science in Engineering 5 (2005) 291–301.
[25] C.H. Chu, J.T. Chen, Automatic tool path generation for 5-axis flank milling based on developable surface approximation, International Journal of Advanced Manufacturing Technology 29 (7–8) (2006) 707–713.
[26] J.H. Lee, Modeling generalized cylinders using direction map representation, Computer-Aided Design and Applications 1 (3) (2004) 541–550.
[27] C.H. Séquin, Rapid prototyping: a 3D visualization tool takes on sculpture and mathematical forms, Communications of the ACM 48 (6) (2005) 66–73.
[28] C.H. Chu, J.T. Chen, Characterizing design degrees of freedom for composite developable Bézier surfaces and their applications in design and manufacturing, Robotics and CIM 23 (1) (2007) 116–125.
[29] G. Farin, Curves and surfaces for computer aided geometric design, Academic Press, 1997.
[30] J. Monterde, Bézier surfaces of minimal area: the Dirichlet approach, Computer-Aided Geometric Design 21 (2004) 117–136.
[31] H.P. Moreton, C.H. Séquin, Functional optimization for fair surface design, SIGGRAPH (1992) 167–176.